Energy 67 (2014) 319–327

Contents lists available at ScienceDirect

Energy

journal homepage: www.elsevier.com/locate/energy

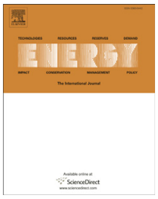

Mass transfer studies during CO_2 gasification of torrefied and pyrolyzed chars

Shubha Shalini Vincent, Nader Mahinpey*, Aqsha Aqsha

Department of Chemical and Petroleum Engineering, Schulich School of Engineering, The University of Calgary, 2500 University Drive NW, Calgary, AB T2N 1N4, Canada

ARTICLE INFO

Article history:
Received 17 August 2013
Received in revised form
11 December 2013
Accepted 15 December 2013
Available online 10 January 2014

Keywords:
Gasification
Torrefied char
Pyrolyzed char
Kinetics
Diffusion
Mass transfer

ABSTRACT

A comparative study on CO_2 gasification kinetics of flax straw char produced by two different processes, namely, torrefaction and pyrolysis was investigated using a TGA (thermogravimetric analyzer). The objective of this research was to investigate the diffusion and surface reactions that occur during the CO_2 gasification of the torrefied and pyrolyzed char particles. Gasification experiments were carried out at four different gasification temperatures from 750 to 900 °C and for different particle sizes (<90 μm −925 μm). The effects of temperature, particle size, and the char type on the rate of CO_2 gasification were determined. The 50% conversion rate showed an increase in the reactivity values, along with an increase in the temperature, and decreased with an increase in the particle size for both the char types. The diffusional parameters such as effective diffusivity, effectiveness factor, and the DLI (diffusion limitation index) were calculated from the experimental data for both the char types. BET (Brunauer-Emmett-Teller) analysis and SEM (Scanning Electron Microscopy) analysis were performed to determine the surface area and to study the structural morphology of the char types. Torrefied char had a greater surface area than the pyrolyzed char.

© 2013 Elsevier Ltd. All rights reserved.

1. Introduction

Biomass is a cheap and renewable energy source. It is considered to be a carbon neutral energy source as well [1]. The thermo–chemical pretreatment of biomass samples such as the torrefaction process, produces a char that is high in carbon content, low in moisture and volatile contents. Also, the torrefaction process increases the energy density and bulk density of the resultant char and, thus reduces storage and transportation costs [2]. The torrefied char possesses high process efficiency (94%) compared to pelletization (84%) and the pyrolysis process (64%). Hence, the torrefaction process is potentially a viable pre-treatment method for improving the properties of biomass samples and their gasification efficiency [3]. The gasification of the solid char that is produced using the thermo–chemical pretreatment methods is endothermic in nature and is a slow process. Gasification of the biomass char can be performed either by using CO_2, H_2O or O_2 [4]. The present study is conducted on CO_2 gasification and the advantage of using CO_2 as a gasifying agent is to recycle the CO_2 that is produced during the pretreatment processes and to convert it into a useful form of gas [5]. Gasification is one of the simplest ways for the production of synthesis gas (CO and H_2) and the process also helps in the production of mechanical and electrical energy [6].

The gasification of the biomass char is a gas–solid reaction and it is usually rate limited. Hence, determination of the gasification rate of the biomass char is one of the most important factors for the design of a gasifier, as it provides information about the volume required by the gasifier to carry out the gasification process [7]. The other physical parameters that influence the gasification rate are the operating temperature, partial pressure of the gasifying agent, particle size of the char, surface area and porosity of the char [8].

The CO_2 gasification kinetics of the biomass char provides valuable information that is useful for the optimum design, operation and modeling of a gasifier [9,10]. The gasification kinetics data is usually determined by a TGA (Thermogravimetric Analyzer) and the findings may deviate from data observed when using commercial reactors [11,12].

The process of carrying out gasification of the torrefied char is similar to the two stage pyrolysis–gasification reaction. The pyrolysis–gasification and torrefaction–gasification processes differ in two aspects. First, the temperature range of the torrefaction process is between 200–300 °C, where the pyrolysis of celluloses is

---

* Corresponding author. Tel.: +1 403 210 6503; fax: +1 403 284 4852.
E-mail address: nader.mahinpey@ucalgary.ca (N. Mahinpey).

0360-5442/$ – see front matter © 2013 Elsevier Ltd. All rights reserved.
http://dx.doi.org/10.1016/j.energy.2013.12.034

minimized and, thus, tar formation is prevented. Second, the heat required for the torrefaction process is less than the pyrolysis process at high temperature.

When the biomass samples undergo rapid heating (pyrolysis) the volatiles that are released are intensified. The effect is a change in the biomass structure and an increase in the pore surface area of the char produced. This phenomenon in turn increases the reactivity of the resultant char [13]. During the torrefaction process the volatile release is controlled under slow heating rate conditions. The char produced by the torrefaction process is expected to exhibit a higher reactivity [14]. The reactivity of the char is dependent on a number of factors namely, the nature and internal structure of the carbonaceous material. The internal structure of the pores and the size of each pore determine the available surface area for the movement of the reactants and products into and out of the surface of the char particle. This process determines the rate of reaction [15]. Reactivity is also dependent on the chemical structure and the inorganic materials that are present in the sample. However, the properties of the reaction from internal pores are very difficult to measure and vary widely with the level of conversion of the char. Thus, the kinetic model is based on global reactivity that takes into account the interaction between the solid (char) and the gas (gasifying agent) [16].

The reactivity that is calculated using the TGA may differ from that calculated using commercial reactors. In commercial reactors, the fuel particles undergo rapid heating during the devolatilization process, which may cause numerous problems such as, uneven temperature distribution along the length of the reactor, and uncertainty in the desirable reaction temperature and reaction time [7]. However, the reactivity calculated using the TGA provides valuable information about the diffusion effects that take place during the char gasification inside a gasifier. In the TGA experiments, a few milligrams of the sample are placed in a sample holder and the gasifying agent (gas) flows across the mouth of the crucible at known concentration and temperature, and thus a stagnant gas region exists between the bulk of the gas, and the upper surface of the sample that is placed in the sample holder, and in the void space around the char particles through, which the gasifying agent should diffuse to reach the external structure of the pores of the char particles.

The steps that occur during the TGA gasification experiments are: 1. External mass and heat transfer: the transfer of the gasifying agent and heat from the bulk of the gas to the external layer of the char particle that is placed in the sample holder. 2. Internal mass and heat transfer: diffusion of the gasifying agent and heat from the external layer into the bed of the char sample. 3. Pore diffusion: diffusion of the gasifying agent and heat from the bed of char sample into the interior of the char particle. During this stage effective conduction of heat occurs through the porous char particle. 4. The final step is the surface chemical reaction. During this final stage, adsorption of CO_2 and desorption of CO from the pores to the external surface of the char particle occurs. This entire gasification process which is carried out using a TGA, may affect the rate of gasification. This should be taken into account when interpreting the results for determining the kinetic parameters [8].

Gasification of torrefied biomass samples was performed by Prins et al. [17]. Their study focused on finding the advantages of the torrefaction process prior to the gasification process for three different gasification configurations: air-blown gasification of wood, air-blown gasification of torrefied wood, and oxygen-blown gasification of torrefied wood. The comparison of their energy efficiency was the focal point of the study. Chen et al. [2] also studied the effects of torrefaction pre-treatment on the gasification process. They examined the characteristics of the torrefaction process, properties of the torrefied products, and the effect of the torrefaction process on the gas composition, cold gas efficiency, and gasification efficiency.

Although numerous studies have been conducted on the CO_2 gasification of the biomass char that is produced by the pyrolysis process, very little research has been done on the CO_2 gasification of torrefied char. Also lacking, are the gasification studies of torrefied char in comparison to pyrolyzed char by CO_2 gasification and the mass-transfer effects that occur during the CO_2 gasification of torrefied char. The present work aims to study the comparison of flax straw char–CO_2 gasification for the chars that are produced by torrefaction and pyrolysis processes. The major goal of this work was to study the gas diffusion and surface reactions that occur in the torrefied and pyrolyzed char during CO_2 gasification, and to determine the effect of temperature and char particle sizes (torrefied and pyrolyzed) on the rate of char gasification.

2. Experimental

2.1. Pyrolysis and torrefaction experiments

Flax straw used for this study was obtained from a farm in Saskatchewan, Canada. The flax straw was ground and sieve analysis was performed to obtain average particle sizes of <90 μm, 287, 512, 725 and 925 μm. Torrefaction and pyrolysis processes were carried out in a split tubular furnace. The reactor used was 25 cm long and had an inner diameter of 4 cm. About 8 g of the flax straw sample was loaded into the reactor at the beginning of each run. Nitrogen gas was used as a carrier gas, at a flow rate of 50 ml/min.

The torrefaction process was carried out at 300 °C. When the furnace reached the desired temperature, the sample was held at that temperature for 60 min. Similarly, the pyrolysis process was carried out at 500 °C and the sample was held at that temperature for 60 min. Once both the processes were complete, the reactor was allowed to cool down to room temperature and the char was collected and stored in desiccators. Similar procedure was followed to produce char using different particle sizes.

2.2. Char gasification

A TGA was used to perform the gasification experiments. A 10 mg char sample was placed in a ceramic crucible and was heated from room temperature to four different gasification temperatures ranging from 750 to 900 °C using nitrogen gas at a flow rate of 45 ml/min. The sample was held at the selected temperature for 5 min in order to obtain a constant weight. The sample was also held at the gasification temperature for a further 45 min to allow for complete gasification to take place. For this 45 min period, the gas used was switched to CO_2 at a flow rate of 45 ml/min.

3. Results and discussion

3.1. Intrinsic kinetics

In order to perform intrinsic kinetic studies, a very fine, powdery torrefied and pyrolyzed char particle size of <90 μm was chosen. The rate equation used is as follows:

$$r = \frac{dX}{dt} = k(1-X)^n \quad (1)$$

Solving the above equation, we get

$$\ln(r) = \ln(k) + n\ln(1-X) \quad (2)$$

where X is conversion (g), k is rate constant (s^{-1}), n is order of reaction that later will be determined, and r is rate of the reaction

(s^{-1}). From the experimental data, plots of ln(r) vs ln($1-X$) for four different gasification temperatures were plotted. The slope of the plot is equal to the order of reaction and its intercept is equal to the rate constant k. From the rate constant values at four different gasification temperatures, the activation energy was calculated using the Arrhenius equation. i.e.,

$$k = Ae^{\left(-\frac{E}{RT}\right)} \tag{3}$$

Taking logarithm on both sides, we get,

$$\ln(k) = \ln(A) - \frac{E}{RT} \tag{4}$$

where, A is pre-exponential factor [s^{-1}], E is activation energy [kJ/mol], R is Ideal gas constant [kJ/mol K] and T is temperature [K]. The ln(k) vs. $1/T$ for four different gasification temperatures was plotted, where its slope is equal to the activation energy and intercept corresponds to the pre-exponential factor. Figs. 1 and 2 show the Arrehenius plots for torrefied and pyrolyzed char. The obtained rate equation for torrefied (Eqn. (5)) and pyrolyzed (Eqn. (6)) char is as follows:

$$r = 95742\,\exp\left(\frac{-150}{RT}\right)(1-X)^{1.09} \tag{5}$$

$$r = 49290\,\exp\left(\frac{-243}{RT}\right)(1-X)^{0.89} \tag{6}$$

Since the gasification temperatures were in the lower range (750–900 °C) and the particle size used was <90 μm, the kinetic parameters that were calculated are considered intrinsic [16]. The order of the reaction was 1.09 for torrefied char and 0.89 for pyrolyzed char, and their activation energies were 150 kJ/mol and 243 kJ/mol, respectively. This variation in the activation energy and order of the reaction was due to the difference in the compositions of ash and its catalytic effect on the gasification of the char samples. The activation energy obtained for torrefied char was rather low when compared to the activation energy obtained for pyrolyzed char. The activation energy obtained for other pyrolyzed biomass chars, such as spruce and birch are 220 kJ/mol and 215 kJ/mol, respectively [8]. These activation energies are comparable with the activation energy obtained for the pyrolyzed flax straw char. For particle sizes other than <90 μm, the obtained activation energy for both torrefied and pyrolyzed char were similar in range.

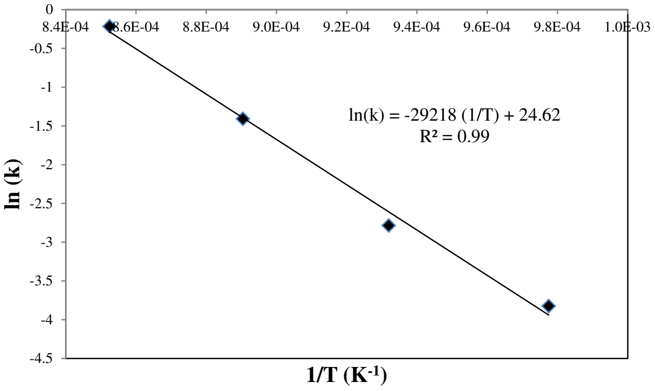

Fig. 1. Arrhenius plot of torrefied char particle size of <90 μm.

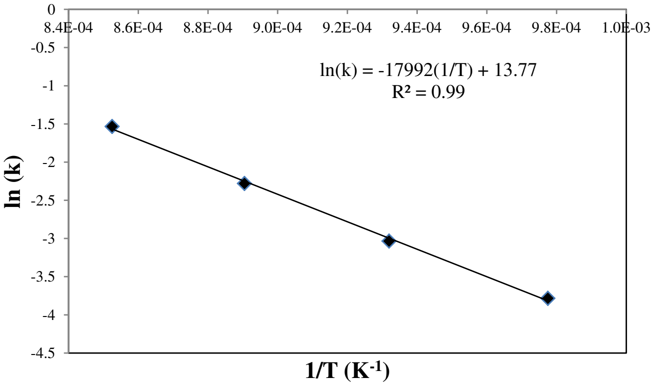

Fig. 2. Arrhenius plot of pyrolyzed char particle size of <90 μm.

3.2. SEM (scanning electron microscopy) analysis of the char particles

SEM analysis provides information about the structural changes that take place on the raw biomass char during the torrefaction and pyrolysis processes. Fig. 3(a), (b), and (c) show the SEM analysis results of raw biomass, pyrolyzed and torrefied char particles respectively. An increase of temperature to the raw flax straw biomass causes the chemical bonds to break and this, in turn, breaks the fibrous structure of the raw flax straw biomass and increases the pores in the char particles. However, this effect was most prominent for torrefied char than pyrolyzed char [18].

Tables 1and 2 show the BET (Brunauer-Emmett-Teller) surface areas of the torrefied and pyrolyzed chars. During the BET analysis, torrefied char particles exhibited higher surface area than pyrolyzed char particles. This difference in the surface areas was possibly due the difference in the compositions and difference in the distribution of lignocellulosic materials in the char particles. Surface area has a significant effect on the reactivity values of both the torrefied and pyrolyzed char. As the surface area decreased with an increase in the particle size, the reactivity of both the torrefied and pyrolyzed char particles decreased. However, torrefied char has a higher reactivity than pyrolyzed char, which was due to the larger surface area of torrefied char [19].

3.3. Effect of gasification temperature on torrefied and pyrolyzed char

Fig. 4 illustrates the char conversion vs. time plot for torrefied char for each gasification temperature studied (750, 800, 850 and 900 °C) and for the different particle sizes studied. Tables 3 and 4 present the proximate and ultimate composition analysis values of the torrefied and pyrolyzed char. The conversion is calculated from the experimental data using the equation

$$X = \frac{w_o - w_t}{w_o - w_f} \tag{7}$$

where, w_o is initial weight of the sample, w_t is weight of the sample at time t (minutes) and w_f is final weight of the sample on ash free basis.

It is clear from the graph that as the gasification temperature increased, the rate of char conversion shifted to a higher degree of conversion. At a lower gasification temperature of about 750 °C the reaction was very slow, and only about 70% of the conversion was achieved for a residence time of 45 min. Further, as the gasification temperature was increased to about 900 °C the reaction was faster, and complete conversion was achieved in the same duration of

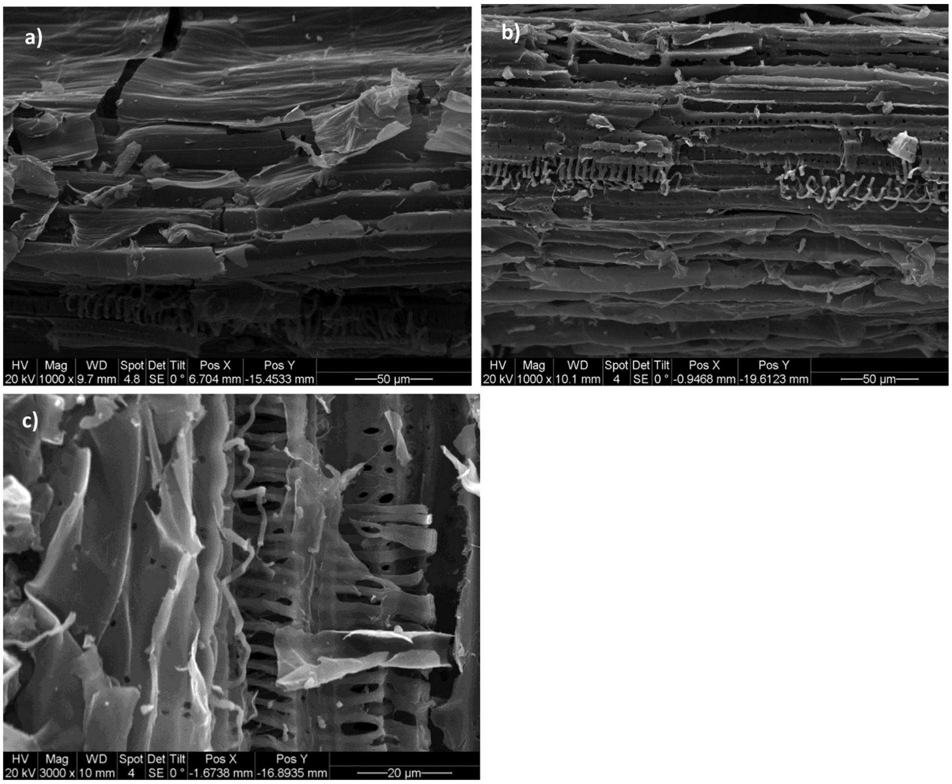
a)
HV | Mag | WD | Spot | Det | Tilt | Pos X | Pos Y
20 kV | 1000 x | 9.7 mm | 4.8 | SE | 0 ° | 6.704 mm | -15.4533 mm
50 μm
b)
HV | Mag | WD | Spot | Det | Tilt | Pos X | Pos Y
20 kV | 1000 x | 10.1 mm | 4 | SE | 0 ° | -0.9468 mm | -19.6123 mm
50 μm
c)
HV | Mag | WD | Spot | Det | Tilt | Pos X | Pos Y
20 kV | 3000 x | 10 mm | 4 | SE | 0 ° | -1.6738 mm | -16.8935 mm
20 μm

Fig. 3. SEM images (a) Raw flax straw (b) Pyrolyzed flax straw char (c) Torrefied flax straw char.

45 min. This trend was observed for all the particle sizes. By taking the experimental reactivity R_{50} (reactivity at 50% conversion) values for all the particles sizes, and for all the gasification temperatures studied, the trend observed is validated. The reactivity is calculated from the experimental data and the equation used to calculate the reactivity is as follows [20],

$$R = \frac{1}{1-X}\frac{dX}{dt}\left[s^{-1}\right] \tag{8}$$

Table 5 shows the reactivity values for different gasification temperatures and for different particle sizes. It can be observed from Table 5, that the reactivity value increases with an increase in the gasification temperature, and moderate to no difference in the reactivity values was observed with an increase in the particles size.

Table 1
BET surface area of torrefied char.

d_p (μm)	Surface area (m^2/g)	Average pore diameter (A°)
<90 μm	1.4844	106.8
287 μm	0.9046	125.7
512 μm	0.7122	129.1
725 μm	0.6066	117.2
925 μm	0.5924	117.5

Table 2
BET surface area of pyrolyzed char.

d_p (μm)	Surface area (m^2/g)	Average pore diameter (A°)
<90 μm	0.589	120.5
287 μm	0.3101	184.0
512 μm	0.171	281.2
725 μm	0.0859	304.4
925 μm	0.0789	325.7

These results coincide with the results reported by other researchers [16,7] for pyrolyzed char.

Fig. 5 illustrates the char conversion vs time plot for pyrolyzed char for different gasification temperatures and for different particle sizes. The pyrolyzed char exhibited similar trends related to char conversion as the torrefied char. At a lower gasification temperature of about 750 °C, the pyrolyzed char achieved a conversion rate of 80%, for the residence time of 45 min. Complete conversion was achieved at a higher gasification temperature of 900 °C. However, at the higher gasification temperature, the torrefied char required less time to reach complete conversion than the pyrolyzed char. Table 6 provides the reactivity values for the pyrolyzed char for different gasification temperatures and for different particle sizes. The reactivity values of the pyrolyzed char followed a trend similar to the torrefied char. However, the calculated reactivity value was higher for the torrefied char than the pyrolyzed char and hence at a higher gasification temperature, the reaction was faster for torrefied char than pyrolyzed char.

3.4. Effect of torrefied and pyrolyzed char particle size on CO_2 gasification

Fig. 4 shows the char conversion vs. time plot for different particle sizes of torrefied char, for different gasification temperatures. The particle size of <90 μm achieved the greatest char conversion when compared to the other particle sizes that were studied. At a lower gasification temperature of 750 °C, the maximum conversion obtained for fine powder particles was 98%, for all the other particle sizes it was around 70% at the same residence time of 60 min. This may be due to the larger total surface area of the fine powder particles collectively. This effect of particle size was verified when reviewing the experimental reactivity data. Table 5 shows the reactivity data at different gasification temperatures for all the particle sizes studied. The reactivity increased

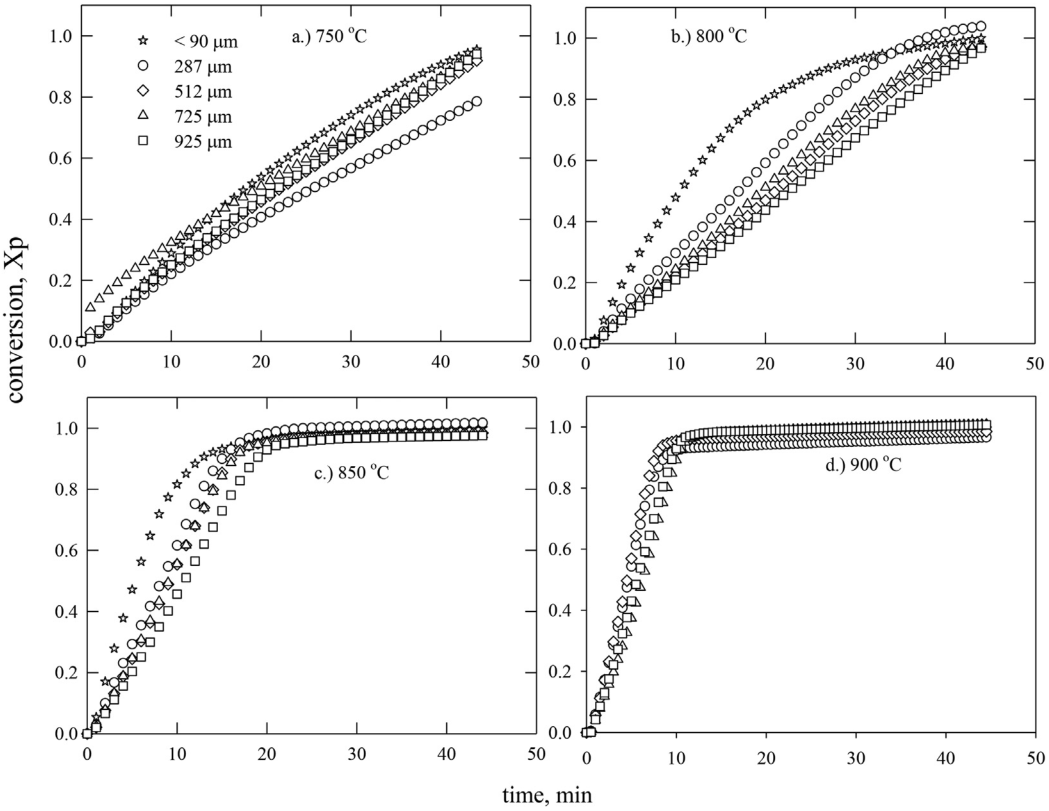

Fig. 4. Conversion vs time plot for torrefied char at different gasification temperatures and at different particle sizes.

with an increase in temperature. There was very little decrease, and constant reactivity values were observed with an increase in the particle sizes thereby showing that intra-particle diffusion is limiting the rate of reaction for larger particle sizes.

Char conversion vs time plots for different gasification temperatures and for different particle sizes of the pyrolyzed char are shown in Fig. 5. Among the various particle sizes studied, the smallest particle size (<90 µm) attained the highest char conversion of 90%, while the largest particle size (925 µm) achieved the lowest conversion of about 80% at the same gasification temperature of 750 °C. For pyrolyzed char, a low rate of char conversion was observed for the higher particle size of 925 µm at all the gasification temperatures studied. This trend was confirmed when reviewing all the experimental reactivity data. In Table 6, the reactivity data at various gasification temperatures and for all the pyrolyzed char particle sizes are summarized.

Figs. 6 and 7 show the plots of the activation energy vs the particle size for torrefied and pyrolyzed char. It is clear from the graph that the physical effects such as growing alkali concentration and phase change that occur during the gasification process are prominent at higher gasification temperatures and for larger particle sizes [11]. With an increase in the particle size, the surface area and rate of reaction decrease dramatically. This phenomenon, in turn, indicates that for larger particle size, the intra-particle concentration gradient exists, and, thereby, creates mass-transfer limitations [11]. Thus, with an increase in the particle size, the activation energy decreased for both the torrefied and pyrolyzed char particles. However, the activation energy for the particle sizes of 725 and 925 µm of the torrefied char were in close range, while, a consistent decrease in the activation energy with an increase in the particle size was observed for pyrolyzed char.

Table 3
Ultimate and proximate analysis of torrefied char.

	Ultimate analysis					Proximate analysis			
Material	C	H	N	S	Moisture	Ash	Volatile	FC	Heating value (kJ/kg)
Torrefied char	61.4	4.82	0.60	0.81	0.12	2.92	52.0	45.2	24,261

Ultimate analysis error ± 0.001, proximate analysis error ± 0.01, heating value error ± 0.001.

Table 4
Ultimate and proximate analysis of pyrolyzed char.

	Ultimate analysis					Proximate analysis			
Material	C	H	N	S	Moisture	Ash	Volatile	FC	Heating value (kJ/kg)
Pyrolyzed char	45.24	6.25	1.01	1.18	8.4	2.4	78.8	18.3	18,120

Ultimate analysis error ± 0.001, proximate analysis error ± 0.01, heating value error ± 0.001.

Table 5
Experimental reactivity of torrefied char.

	Reactivity, R_{50} (s^{-1})			
	750 °C	800 °C	850 °C	900 °C
<90 µm	0.031	0.069	0.147	0.249
287 µm	0.013	0.049	0.093	0.206
512 µm	0.012	0.052	0.123	0.225
725 µm	0.012	0.051	0.121	0.229
925 µm	0.014	0.052	0.120	0.227

Uncertainty in $R_{50} \pm 0.005$[s^{-1}].

3.5. *Effectiveness factor*

Effectiveness factor is used to measure how much the rate of reaction is lowered due to the resistance to pore diffusion [16]. It is also defined as the ratio of the actual conversion (X_p) to the conversion obtained when there is no external, or intra-particle gradient observed ($X_\mathrm{p,int}$) at any instant of time.

$$\eta_\mathrm{R}((t)) = \frac{X_\mathrm{p}(t)}{X_\mathrm{p,int}(t)} \tag{9}$$

where, X_p is conversion of particles (with diffusion effects) at any time t, and $X_\mathrm{p,int}$ is conversion of char particle size of <90 µm.

This effectiveness factor was introduced by Ramachandran et al. [21]. The effectiveness factor is useful for directly predicting the diffusion effects from the experimental conversion vs time data [7]. The effectiveness factor presented in this work is calculated from the experimental conversion vs time curve [21]. Figs. 8 and 9 show a plot of the effectiveness factor vs the different particle sizes for the torrefied and pyrolyzed biomass char gasification. The effectiveness factor for the particle size of <90 µm was 0.98 at all gasification temperatures studied for torrefied char and 1.0 for the pyrolyzed char particles. The diffusion path increases with an increase in the particle size and hence, no significant drop in the effectiveness factor was observed for particle sizes other than <90 µm. This effect was similar for both the torrefied and pyrolyzed char types. For effectiveness factors close to unity, the entire volume of the char particles reacts at a higher rate, because the reactant is able to diffuse quickly into the pores of the char particles. Thus, when the diffusion rate is faster than the reaction rate and the effectiveness factor is close to unity, the conversion of char particle is reaction limited. For effectiveness factor lower than unity, the char particles react at a lower rate as the gasifying agent cannot penetrate into the interior of the char particles significantly. Thus, when the diffusion rate is lower than the reaction rate, the conversion of the char particles is diffusion limited [22]. It is clear from Figs. 8 and 9 that the conversions of larger particle sizes of both the torrefied and pyrolyzed char are diffusion limited and the conversion for the particle size of <90 µm is reaction limited. The maximum effectiveness factor observed for the torrefied and pyrolyzed char was at 750 °C, for all the particle sizes studied. With an increase in the temperature, the physical effects become prominent and thus, the effectiveness factor decreased with an increase in the gasification temperature [16]. The effectiveness factor obtained at higher gasification temperatures for all the particle sizes included in this study was almost equal for the torrefied chars, and a moderate decrease in the effectiveness factor was observed for pyrolyzed chars. In the present study, the char conversion for particle sizes >90 µm is governed by intra pore diffusion and hence, the effectiveness factor depends on the structure, volume and shape of each of pores which vary for each of the particle sizes. This was the reason for the variation in the effectiveness factor between

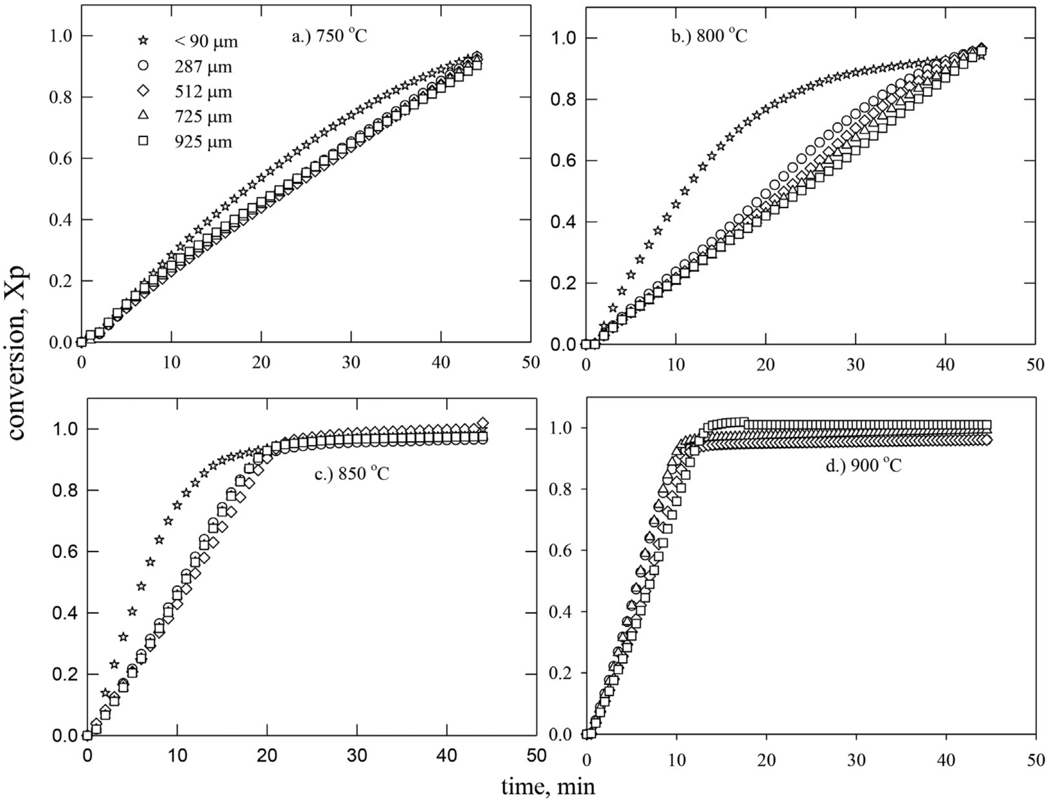

Fig. 5. Conversion vs time plot for pyrolyzed char at different gasification temperatures and at different particle sizes.

Table 6
Experimental reactivity of pyrolyzed char.

	Reactivity, R_{50} (s^{-1})			
d_p (μm)	750 °C	800 °C	850 °C	900 °C
<90 μm	0.041	0.070	0.214	0.319
287 μm	0.016	0.054	0.110	0.213
512 μm	0.015	0.048	0.107	0.195
725 μm	0.013	0.046	0.109	0.176
925 μm	0.009	0.035	0.067	0.155

Uncertainty in $R_{50} \pm 0.005[s^{-1}]$.

torrefied char and pyrolyzed char. Also, torrefied char particle sizes had almost similar reactivity, while, for the pyrolyzed char the reactivity decreased considerably (Tables 5 and 6). Similar response was obtained by other studies [11,16] for pyrolyzed char, while the effect of torrefied char particle sizes, investigated in this study, has not been reported yet. Thus, our study would serve as a basis for future research investigations.

Tables 7 and 8 show the effective diffusivity values for torrefied and pyrolyzed char. These values are calculated according to the methods suggested by Gomez-Barea et al. [7]. Appendix-A provides an explanation of the equations used to calculate the effective diffusivity. The effective diffusivity values increased considerably with an increase in the particle size and a moderate increase was observed with an increase in the gasification temperature for the torrefied char. The effective diffusivity values were observed to show similar trends for the pyrolyzed char gasification. As the particle size increases, an increase in the pore diameter and a decrease in the surface area of the char particles were observed. As the particle sizes chosen for the present study were average particle sizes, there exists a difference in the pore structure of the individual particles. This may be the reason for observing an increasing trend in the effective diffusivity with an increase in the particle sizes. The diffusivity value obtained for torrefied char was higher when the particle size was 925 μm, and the diffusivity value was 2.0 m^2/min. For pyrolyzed char, the maximum diffusivity value observed was also at the larger particle size of 925 μm. However, the diffusivity value was around 5 m^2/min. Thus the pyrolyzed char has a faster diffusion of CO_2 into the pores of the char than the torrefied char.

3.6. DLI (diffusion limitation index)

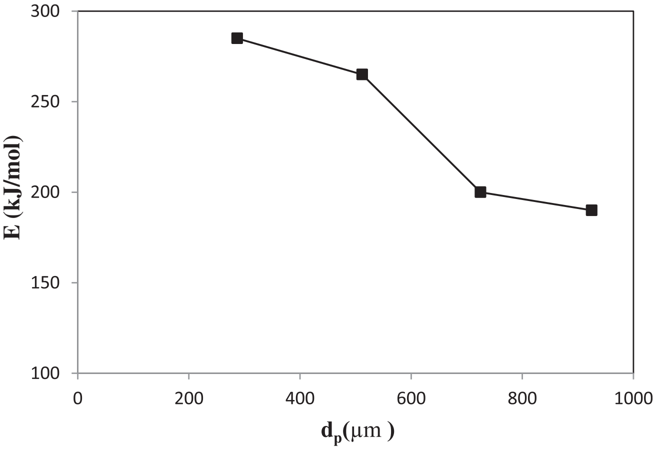

Fig. 6. Activation energy (E) vs particle sizes (d_p) plot for torrefied char.

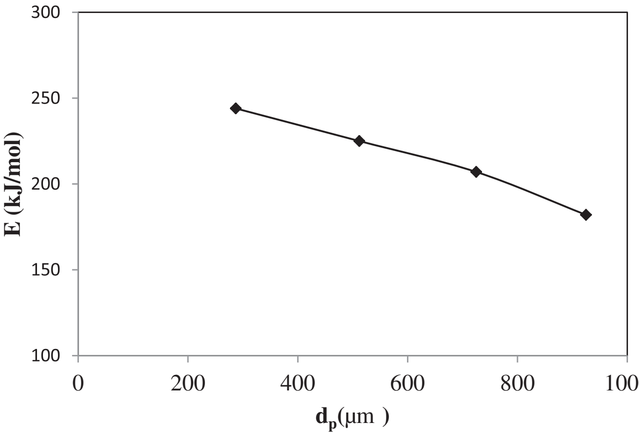

Fig. 7. Activation energy (E) vs particle sizes (d_p) plot for pyrolyzed char.

Convective mass transfer is not as effective as diffusion mass transfer. However, its effects on the gasification rate must be determined. In order to account for this effect, DLI is calculated for each experiment as follows [7],

$$\mathrm{DLI} = \frac{\text{observed gasification rate } \left(\frac{1}{s}\right) \text{ at } X = 50\%}{\text{maximum molecular diffusion rate } \left(\frac{1}{s}\right)} = \frac{r_{\mathrm{obs}}}{r_{\mathrm{D,e}}} \tag{10}$$

While observed gasification rate is calculated using the equation below [7],

$$r_{\mathrm{obs}} = \frac{R_{50}w}{M_C} \tag{11}$$

The external diffusion is estimated by assuming that the movement of the reactant into the sample takes place by Fick's molecular diffusion and, therefore, the length of the diffusion path is equal to half the radius of the hemisphere of the sample tray (Ollero et al., 2003). The molecular diffusion is calculated according to the following equation [7],

$$r_{D_m} = c_0 D_m \pi d_t \tag{12}$$

The calculated DLI values up to 0.1 are considered as acceptable range for the CO_2 gasification process. The calculated DLI values for the particle size of <90 μm for the torrefied and pyrolyzed char are

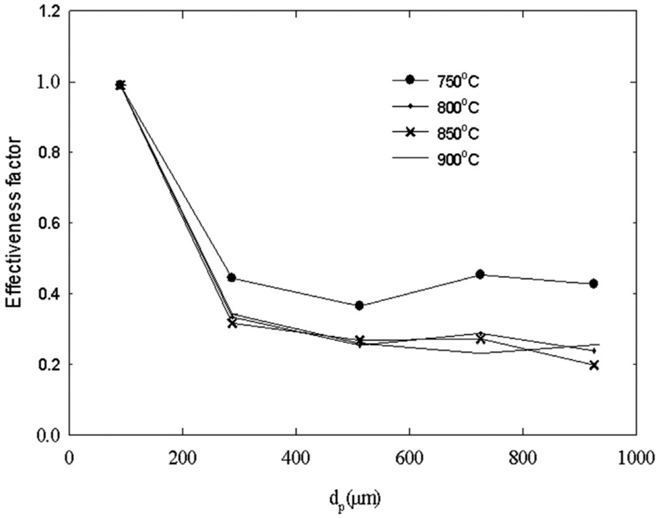

Fig. 8. Plot of Effectiveness factor vs particle size for torrefied char.

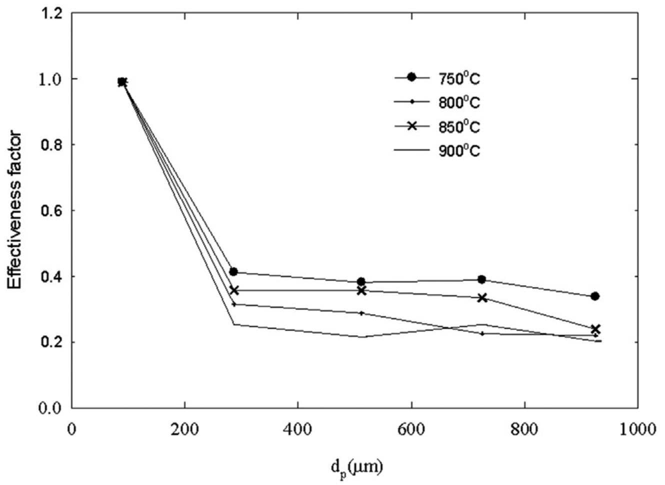

Fig. 9. Plot of Effectiveness factor vs particle size for pyrolyzed char.

Table 7
Effective diffusivity values of torrefied char.

	Effective diffusivities, D_e (m^2/min) × 10^{-4}			
d_p (μm)	750 °C	800 °C	850 °C	900 °C
<90 μm	0.0036	0.0037	0.0038	0.00388
287 μm	0.040	0.041	0.0421	0.0432
512 μm	0.286	0.293	0.300	0.307
725 μm	0.933	0.958	0.981	1.000
925 μm	1.920	1.970	2.020	2.070

Uncertainty in D_e ± 0.005[s^{-1}].

found in Table 9. It can be noted from Table 9, that the DLI values for the torrefied and pyrolyzed char for gasification temperatures of 750 and 800 °C are within the range of 0.1. At higher gasification temperatures of 850 and 900 °C, the calculated DLI values were greater than 0.1, both for the torrefied and pyrolyzed char. This may be due to the uncertainty in the R_{50} values at higher gasification temperatures. Similar results for the DLI values were obtained by Gomez-Barea et al. [7] and Ollero, P et al. [23].

4. Conclusion

Mass transfer and surface reaction were studied for the CO$_2$ gasification of torrefied and pyrolyzed char at different gasification temperatures and particle sizes. The reaction was a first order rate equation with respect to char conversion for both the torrefied and pyrolyzed chars. Maximum char conversion was obtained at a gasification temperature of 900 °C for both the torrefied and pyrolyzed chars and at this temperature of 900 °C the reaction was faster for torrefied char than pyrolyzed char. There was very little change observed for torrefied char in the reactivity values when particle size was increased from the smallest particle size of <90 μm. For the pyrolyzed char, a decrease in the reactivity values was observed with an increase in the particle size. The maximum effectiveness was observed at the lower gasification temperature of 750 °C, for both torrefied and pyrolyzed char. The effectiveness factor decreased with an increase in the temperature and particle sizes and hence it is concluded that diffusion is rate limiting for larger particle sizes for both torrefied and pyrolyzed chars. As the results of this investigation present a novel approach for the study of mass transfer phenomena on the gasification of torrefied char, the outcome will be of vital importance in designing gasification units while the torrefied char is fed. Further studies on the influence of heat transfer on both mass transfer and surface reactions will shed more light on the overall gasification process.

Table 8
Effective diffusivity values of pyrolyzed char.

	Effective diffusivities, D_e (m^2/min) × 10^{-4}			
d_p (μm)	750 °C	800 °C	850 °C	900 °C
<90 μm	0.056	0.0574	0.0587	0.06
287 μm	0.0806	0.0825	0.0845	0.0863
512 μm	0.576	0.591	0.605	0.619
725 μm	2.26	2.32	2.39	2.46
925 μm	4.85	5.03	5.21	5.38

Uncertainty in D_e ± 0.005[s^{-1}].

Table 9
Diffusional limitation index of torrefied and pyrolyzed char for a particle size of <90 μm.

Temperature (°C)	DLI values (torrefied)	DLI values (pyrolyzed)
750	0.047	0.081
800	0.096	0.132
850	0.187	0.149
900	0.374	0.584

Uncertainty in DLI ± 0.001[s^{-1}].

Acknowledgments

We gratefully acknowledge financial support by Natural Science and Engineering Research Council of Canada.

Appendix-A

To calculate effective diffusivity (D_e), two diffusion mechanisms must be taken into account, one inside the porous material (bulk) and second Knudsen diffusion. D_e is calculated according to Bosanquet formula which is as follows:

$$D_e = \frac{1}{(1/D_b) + (1/D_{K_n})} \tag{A.1}$$

where D_b, D_m and D_{K_n} are calculated according to the following equations:

$$D_b = \left(\frac{\varepsilon}{\tau_t}\right)D_m \tag{A.2}$$

$$D_m = 1.4 \times 10^{-5}\left(\frac{T}{273}\right)1.8 \tag{A.3}$$

$$D_{K_n} = \frac{2}{3}\sqrt{\frac{8R_gT}{\pi M_g}}r_p \tag{A.4}$$

where r_p is the porosity ratio and it is estimated as $r_p = 4\varepsilon/S_c$.

References

[1] Demirbas A. Biomass resources facilities and biomass conversion processing for fuel and chemicals. Energy Convers Manag 2001;42(11):1357–78.
[2] Chen Q, Zhou JS, Liu B, Mei QF, Luo ZY. Influence of torrefaction pre-treatment on biomass gasification technology. Energy Sci Technol 2011;56:1449–56.
[3] Uslu A, Faaij APC, Bergman PCA. Pre-treatment technologies and their effect on international bioenergy supply chain logistics. Techno-economic

evaluation of torrefaction, fast pyrolysis and pelletisation. Energy 2008;33:1206–23.

[4] Kannan MP, Richards GN. Gasification of biomass chars in carbon dioxide: dependence of gasification rate on the indigenous metal content. Fuel 1990;69:747–53.

[5] Garcia L, Salvador ML, Arauzo J, Bilbao R. CO_2 as a gasifying agent for gas production from pine sawdust at low temperatures using a Ni/Al co–precipitated catalyst. Fuel Process Technol 2001;69:157–74.

[6] Khalil R, Varhegyi G, Jaschke S, Gronli MG, Hustad J. CO_2 gasification of biomass chars: a kinetic study. Energy Fuel 2009;23:94–100.

[7] Gomez-Barea A, Ollero P, Fernandez-Baco C. Diffusional effects in CO_2gasification experiments with single biomass char particles. 1. Experimental investigation. Energy Fuel 2006;20:2202–10.

[8] Ollero P, Serrera A, Arjona R, Alcantarilla S. Diffusional effects in TGA gasification experiments for kinetics determination. Fuel 2002;81:1989–2000.

[9] Gobel B, Bentzen JD. Dynamic modeling of the two stage gasification process. In: Proceedings of the Fourth Biomass Conference of the Americas, Oakland, CA, USA 1999. pp. 1025–32.

[10] Feng B, Bhatia SK. On the validity of thermogravimetric determination of carbon gasification kinetics. Chem Eng Sci 2002;57:2907–20.

[11] Gomez–Barea A, Ollero P, Arjona R. Reaction–diffusion model of TGA gasification experiments for estimating diffusional effects. Fuel 2005;84: 1695–704.

[12] Yang KL, Yang RT. Absolute rates of the carbon–carbon dioxide reaction. AIChE J 2004;31(8):1313–21.

[13] Di Blasi C. Combustion and gasification rates of lignocellulosic chars. Prog Energy Combust Sci 2009;35(2):121–40.

[14] Fisher EM, Dupont C, Darvell LI, Commandré JM, Saddawi A, Jones JM, et al. Combustion and gasification characteristics of char from raw and torrefied biomass. Bioresour Technol 2012;119:157–65.

[15] Standish N, Tanjung AFA. Gasification of single wood charcoal particles in CO_2. Fuel 1988;67:666–72.

[16] Mani T, Mahinpey N, Murugan P. Reaction kinetics and mass transfer studies of biomass char gasification with CO_2. Chem Eng Sci 2011;66:36–41.

[17] Prins MJ, Ptasinski KJ, Janseen FJJG. More efficient biomass gasification via torrefaction. Energy 2006;31:3458–70.

[18] Dutta S, Wen CY, Belt RJ. Reactivity of coal and char in CO_2 atmosphere. Ind Eng Chem Process Design Develop 1977:20.

[19] Tushar MSHK, Mahinpey N, Murugan P, Mani T. Analysis of gaseous and liquid products from pressurized pyrolysis of flax straw in a fixed bed reactor. Ind Eng Chem Res 2010;49:4627–32.

[20] Hehati M, Laguerie C. Determination of the kinetics of the wood sawdust steam gasification of charcoal in a thermobalance. Entropie 1988;142: 29–40.

[21] Gomez–Barea A, Ollero P, Villanueva A. Diffusional effects in CO_2 gasification experiments with single biomass char particles. 2. Theoretical prediction. Energy Fuel 2006;20:2211–22.

[22] Rawlings JB, Ekerdt JG. Chemical reactor analysis and design fundamentals. 2nd ed. Nob Hill Publication; 2011.

[23] Ollero P, Serrera A, Arjona R, Alcantarilla S. The CO_2 gasification kinetics of olive waste. Biomass Bioenergy 2003;24:151–61.

Glossary

Symbol

A: pre-exponential factor (s^{-1})
c_0: initial gas concentration (mol/m^3)
d_p: particle size (m)
d_t: crucible diameter (m)
D: diffusion
DLI: diffusion limitation index
ε: char porosity
E: activation energy (kJ/mol)
k: rate constant (s^{-1})
M_g: gas molecular weight (kg/kmol)
M_C: carbon molecular weight (kg/kmol)
η_R: effectiveness factor (Ramachandran)
n: order of reaction
ρ_c: apparent carbon density (kg/m^3)
r: rate of reaction (s^{-1})
r_{obs}: observed gasification rate (kmol/s)
$r_{D,e}$: maximum external diffusion (kmol/s)
$r_{D,i}$: maximum internal diffusion (kmol/s)
r_p: pore radius (m)
R: ideal gas constant (kJ/mol K)
S_c: specific surface area of the char particle (m^2/g)
τ_t: tortuosity
t: time (s)
T: temperature (K)
w: instantaneous char weight (kg)
X: conversion
X_p: global particle conversion

Subscripts

b: bulk diffusion mechanism
e: effective diffusion
f: final
i: instantaneous values
int: intrinsic
K_n: Knudsen diffusion mechanism
m: molecular diffusion
o: initial
t: at time t